Molecular Therapy
Original Article

Gut microbial metabolite hyodeoxycholic acid targets the TLR4/MD2 complex to attenuate inflammation and protect against sepsis

Jiaxin Li,[1,2,9] Yuqi Chen,[1,9] Rui Li,[1,9] Xianglong Zhang,[1,9] Tao Chen,[1] Fengyi Mei,[1] Ruofan Liu,[1] Meiling Chen,[1] Yue Ge,[2] Hongbin Hu,[2] Rongjuan Wei,[1] Zhenfeng Chen,[1] Hongying Fan,[3] Zhenhua Zeng,[2] Yongqiang Deng,[1] Haihua Luo,[1] Shuiwang Hu,[1] Shumin Cai,[2] Feng Wu,[2] Nengxian Shi,[2] Zhang Wang,[4] Yunong Zeng,[1] Ming Xie,[5] Yong Jiang,[1] Zhongqing Chen,[2] Wei Jia,[6,7] and Peng Chen[1,8]

[1]Department of Pathophysiology, Guangdong Provincial Key Laboratory of Proteomics, School of Basic Medical Sciences, Southern Medical University, Guangzhou 510515, China; [2]Department of Critical Care Medicine, Nanfang Hospital, Southern Medical University, Guangzhou 510515, China; [3]Department of Microbiology, Guangdong Provincial Key Laboratory of Tropical Disease Research, School of Public Health, Southern Medical University, Guangzhou 510515, China; [4]Institute of Ecological Sciences, School of Life Sciences, South China Normal University, Guangzhou 510515, China; [5]Department of Urology, Nanfang Hospital, Southern Medical University, Guangzhou 510515, China; [6]Center for Translational Medicine and Shanghai Key Laboratory of Diabetes Mellitus, Shanghai Jiao Tong University Affiliated Sixth People's Hospital, Shanghai 200233, China; [7]School of Chinese Medicine, Hong Kong Baptist University, Kowloon Tong, Hong Kong 999077, China; [8]Microbiome Medicine Center, Zhujiang Hospital, Southern Medical University, Guangzhou 510515, China

Sepsis, a critical condition resulting from the systemic inflammatory response to a severe microbial infection, represents a global public health challenge. However, effective treatment or intervention to prevent and combat sepsis is still lacking. Here, we report that hyodeoxycholic acid (HDCA) has excellent anti-inflammatory properties in sepsis. We discovered that the plasma concentration of HDCA was remarkably lower in patients with sepsis and negatively correlated with the severity of the disease. Similar changes in HDCA levels in plasma and cecal content samples were observed in a mouse model of sepsis, and these changes were associated with a reduced abundance of HDCA-producing strains. Interestingly, HDCA administration significantly decreased systemic inflammatory responses, prevented organ injury, and prolonged the survival of septic mice. We demonstrated that HDCA suppressed excessive activation of inflammatory macrophages by competitively blocking lipopolysaccharide binding to the Toll-like receptor 4 (TLR4) and myeloid differentiation factor 2 receptor complex, a unique mechanism that characterizes HDCA as an endogenous inhibitor of inflammatory signaling. Additionally, we verified these findings in TLR4 knockout mice. Our study highlights the potential value of HDCA as a therapeutic molecule for sepsis.

INTRODUCTION

Sepsis, a syndrome of organ dysfunction due to the dysregulation of host inflammatory responses to systemic infection, is a global healthcare challenge.[1,2] To eliminate invading pathogens, cytokine production is required to activate immune cells that respond to bacterial antigens. However, the overproduction of pro-inflammatory cytokines during the course of infection has been associated with a higher mortality rate in the early stages of sepsis.[3–5] Thus, anti-inflammatory strategies are implemented early in sepsis patients to restore immunological homeostasis.

Over the past few years, the gut microbiota has been extensively investigated in relation to sepsis development.[6–11] Recently, attention has been drawn to the role of metabolites produced by gut microbiota, with mechanistic studies suggesting that specific gut metabolites have excellent anti-inflammatory properties.[12–14] We found that microbiota-derived granisetron has an anti-inflammatory effect, modulates the host immune system, and determines host susceptibility to the development of sepsis in mice,[15] while other reports also showed similar therapeutic benefits of microbial metabolites in sepsis models, including butyrate (short-chain fatty acids),[16] ursodeoxycholic acid,[17] and taurodeoxycholate.[18] These results have provided strong evidence that warrants further investigation of gut microbial metabolites with anti-inflammatory activity as a potential therapeutic option for sepsis. Hyodeoxycholic acid (HDCA, also known as 3α,6α-dihydroxy-5β-cholanic acid) is a secondary bile acid converted by the gut microbiota from the primary bile acids.[19] Our previous

Received 26 August 2022; accepted 19 January 2023;
https://doi.org/10.1016/j.ymthe.2023.01.018.

[9]These authors contributed equally

Correspondence: Zhongqing Chen, Department of Critical Care Medicine, Nanfang Hospital, Southern Medical University, Guangzhou 510515, China.
E-mail: zhongqingchen2008@163.com
Correspondence: Wei Jia, School of Chinese Medicine, Hong Kong Baptist University, Hong Kong 999077, China.
E-mail: weijia1@hkbu.edu.hk
Correspondence: Peng Chen, Department of Pathophysiology, Southern Medical University, Guangzhou 510515, China.
E-mail: perchen@smu.edu.cn

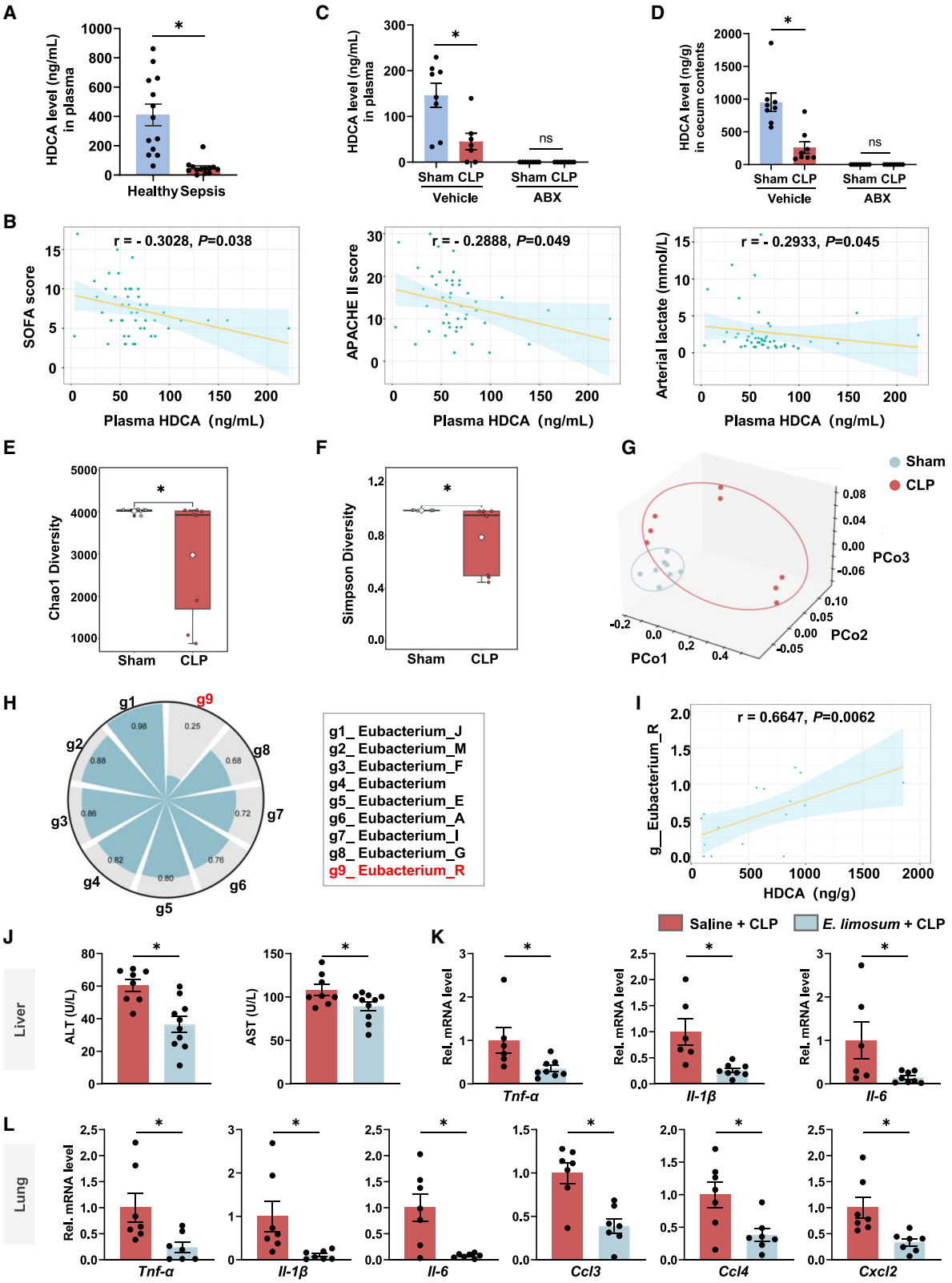

(legend on next page)

study and other laboratories have reported that HDCA is involved in metabolic diseases, with beneficial effects including alleviating hyperglycemia,[20] preventing gallstone formation,[21] suppressing atherosclerosis development,[22] and inhibiting cholesterol levels.[23]

In this study, a lower plasma HDCA level was found in patients with sepsis, and the level of HDCA was negatively correlated with the severity of sepsis. We further identified HDCA as an endogenous antagonist of the Toll-like receptor 4 (TLR4), which suppressed the overproduction of pro-inflammatory factors in response to lipopolysaccharide (LPS) and prevented septic mice from a severe inflammatory reaction, organ damage, or even death. Therefore, we systematically investigated the anti-inflammatory activity of HDCA as well as its mechanistic role in restoring the impaired immune homeostasis associated with sepsis.

RESULTS

Endogenic HDCA level is reduced in septic patients and mice

To understand the potential contribution of HDCA on sepsis, 13 septic patients and 13 age- and gender-matched healthy subjects (Table S1) were recruited, and their plasma HDCA levels were measured. As Figure 1A shows, the plasma HDCA levels in septic patients (48.52 ± 13.14 ng/mL) were significantly lower than those in the healthy subjects (411.50 ± 74.40 ng/mL). We then extended the sepsis cohort to 47 participants (Table S1) and found that, to some extent, the plasma HDCA levels were negatively correlated with the Sequential Organ Failure Assessment (SOFA) scores, the Acute Physiology and Chronic Health Evaluation II (APACHE II) scores, and the arterial lactate levels in septic patients, which are used to determine the disease severity of critical patients (Figure 1B). Furthermore, cecal ligation and puncture (CLP)-induced septic mouse models were established to verify the above finding, as it is considered the standard model for pre-clinical sepsis.[24] As expected, both plasma and cecal HDCA levels significantly decreased in septic mice compared with sham-operated mice (Figures 1C and 1D). In light of these results, HDCA may play a significant role in the pathogenesis of sepsis.

Given that the level of secondary bile acid is mainly synthesized by the gut microbiota,[19] we further investigated the contribution of gut microbes to the level of HDCA by employing antibiotics (ABX)-treated mice. The results affirmed that the level of HDCA cannot be detected (below the minimal detectable concentrations) in the plasma and cecal contents of ABX-treated mice (Figures 1C and 1D), implying that the level of HDCA was generated by gut microbiota in mice. Therefore, we hypothesize that lower levels of HDCA may be associated with lower relative abundances of gut microbes involved in HDCA production. To address this issue, we performed a metagenomic sequencing analysis of cecal contents obtained from both the sham and CLP groups. As illustrated in Figures 1E–1G, the alpha diversity (Chao1 and Simpson index) of gut microbiota in septic mice was markedly diminished compared with sham-operated mice, and beta diversity (principal coordinate analysis [PCoA]) revealed that the overall microbial composition between sham and sepsis was different. According to the report by Eyssen et al.,[25] a strain of *Eubacterium* (EMBL: AJ238611) isolated from rat gut microflora could produce HDCA *in vitro*; we thus evaluated the relative abundance of genus *Eubacterium* in the cecal contents and found that the relative abundance of the genus *Eubacterium* was remarkably decreased in the CLP group compared with that in the sham group, especially the genus *Eubacterium_R* (Figures 1H and S1A). Regarding the species level, the relative abundances of *Eubacterium_R_sp002493325*, *Eubacterium_R_sp000434995*, *Eubacterium_R_sp003526845*, and *Eubacterium_R_sp000436835* were all substantially lower in the CLP group than in the sham group (Figure S1B). In addition, we evaluated the correlation between the relative abundance of the genus *Eubacterium* and the respective cecal HDCA content in each animal to confirm the key gut microbial members possibly contributing to HDCA level alteration during sepsis in mice. As shown in Figure 1I, the relative abundance of the genus *Eubacterium_R* was positively correlated with the concentration of HDCA. These data demonstrated that sepsis is associated with a lower level of HDCA, which might be closely associated with the decreased abundance of the genus *Eubacterium* during the sepsis challenge.

Since the strain of *Eubacterium_R* is unavailable, to further explore the relationship between *Eubacterium* and HDCA, we supplemented the mice with an available strain of *Eubacterium limosum* ATCC 8486 (*E. limosum*), which was isolated from human intestine.[26] Figure S2 illustrates that the concentration of HDCA in mouse feces was significantly increased after oral inoculation with 1×10^8 colony-forming units (CFU)[27] for 7 days. Our results suggested that *E. limosum* is one

Figure 1. Endogenic HDCA level is reduced in septic patients and mice

(A) The concentration of HDCA in the plasma of humans was determined by liquid chromatography-tandem mass spectrometry (LC-MS/MS) (n = 13 healthy subjects, n = 13 sepsis patients). (B) Scatterplot depicting the statistical correlation of plasma HDCA concentrations with SOFA score, APACHE II score, and arterial lactate levels in septic patients (n = 47 sepsis patients). (C) The concentration of HDCA in the plasma of mice was determined by LC-MS/MS. Mice were treated with water or ABX cocktails for 3 days and subjected to sham-operated and CLP surgery. Plasma was collected 12 h after surgery (n = 15 in the vehicle group, n = 16 in the ABX group). (D) The concentration of HDCA in the cecal contents of mice was determined by LC-MS/MS (n = 16 in the vehicle group, n = 16 in the ABX group). (E and F) Alpha diversity (observed species) in each group was calculated using the (E) Chao1 index and (F) Simpson index (n = 8). (G) Each group's beta diversity (microbial community structures) was calculated using a PCoA score based on the weighted UniFrac distance matrices (n = 8). (H) Ratio of mean relative abundance in the CLP groups compared with the sham groups at the level of the genus *Eubacterium* shown in the blue area. The black line on the circle represents a ratio equal to 1. The specific ratios of the CLP versus sham group are shown on the graph (n = 8). (I) Scatterplot depicting the statistical correlation between HDCA level in the cecum contents and the relative abundance of genus *Eubacterium_R* (n = 16). (J) Plasma ALT and AST levels (n = 8–10). (K) Inflammatory cytokine mRNA levels of *Tnf-α*, *Il-1β*, and *Il-6* in liver tissue (n = 6–8). (L) Inflammatory factor mRNA levels in lung tissue (n = 7). *$p < 0.05$ (unpaired two-tailed Student's t test in A, C, D, and J–L; Wilcoxon rank-sum test in E and F; PERMANOVA in G; Spearman rank-order correlation test in B and I; mean ± SEM).

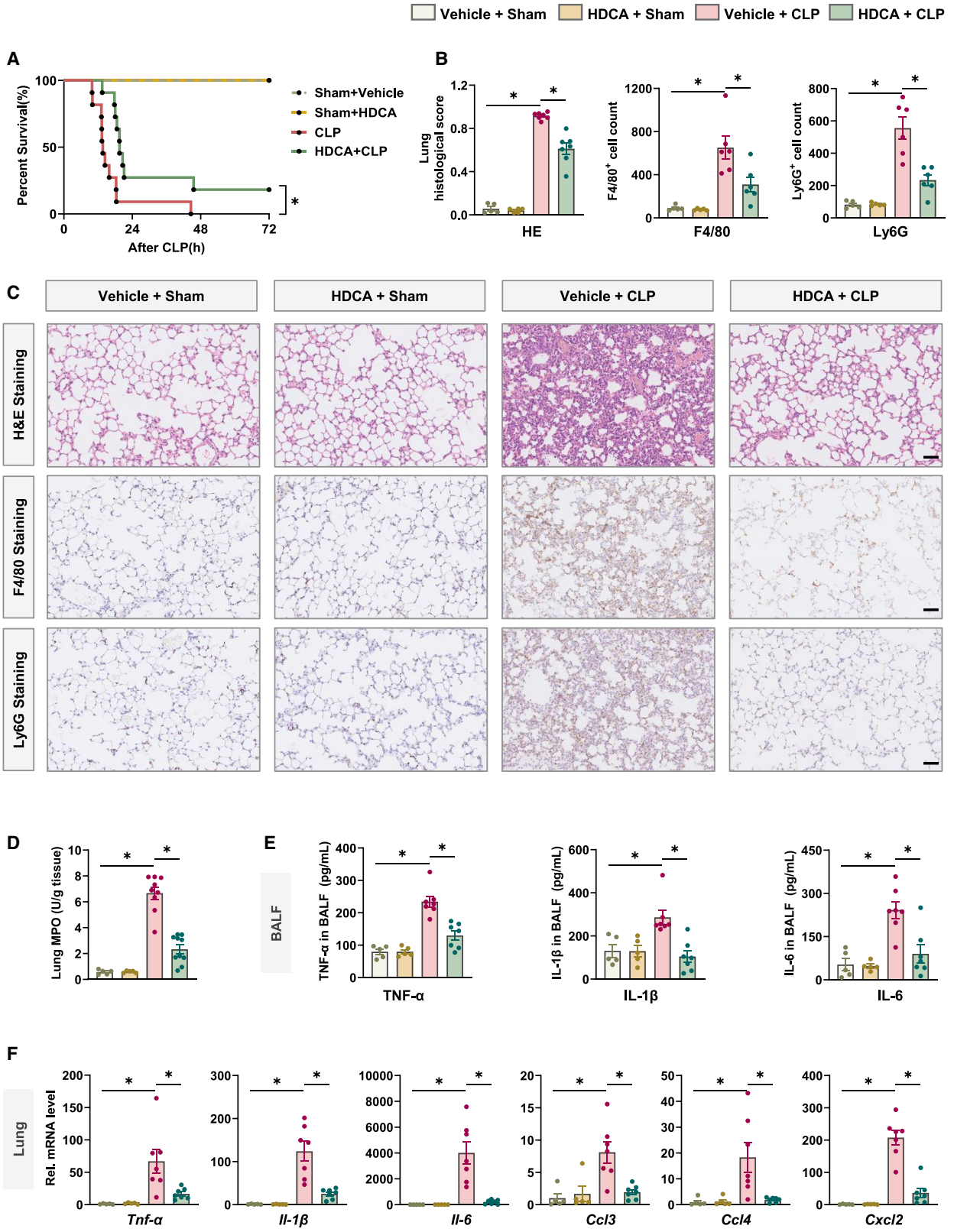

(legend on next page)

of the gut bacteria that intrinsically produce HDCA. Therefore, we wondered whether *E. limosum* could provide a preventive effect in response to polymicrobial sepsis. To investigate this, *E. limosum* was orally inoculated for 7 days before CLP and the effects of anti-inflammatory and organ protection were then determined. Compared with the saline group, *E. limosum* lowered plasma alanine aminotransferase (ALT) and aspartate transaminase (AST) levels and reduced the severity of liver and lung inflammation, as revealed by reduced inflammatory cytokine levels (Figures 1J–1L). These results suggested that *E. limosum*, a potential HDCA-producing bacterium, may, to some extent, exert anti-inflammation effects in septic mice and protect the mice from septic injury.

HDCA protected mice from polymicrobial sepsis

To further explore whether HDCA participates in sepsis development, mice were treated with HDCA (20 mg/kg) for 2 h before CLP surgery. We detected the concentration of HDCA in cecal contents at 12 h after surgery and found that HDCA treatment restored and maintained the cecal HDCA concentrations after CLP surgery (1,401 ± 258.4 ng/g) comparable with physiological concentrations (950.9 ± 139.5 ng/g, $p = 0.17$) (Figure S3). In addition, we observed that HDCA treatment effectively prolonged the mice survival rate in both CLP-induced and LPS-induced sepsis compared with those without treatment (Figures 2A and S4). Given that the lung is the organ most susceptible to sepsis,[28] lung tissue injury assessment was conducted to determine the severity of organ inflammatory response. As shown in Figures 2B and 2C, the septic mice suffered from severe lung injury characterized by thickening of the alveolar septum, cellular infiltration, hemorrhage, and edema. Nevertheless, HDCA-treated septic mice showed less cellular infiltration and protein fragment deposition, along with lower alveolar septal thickening and lung injury scores. In addition, the infiltration of inflammatory cells was assessed by F4/80 and Ly6G staining immunohistochemically. We found that a large number of $F4/80^+$ macrophages and $Ly6G^+$ neutrophils were detected in the CLP group and were significantly reduced by the HDCA treatment. To further assess the magnitude of lung inflammation, myeloperoxidase (MPO) activity, pro-inflammatory cytokine levels in bronchoalveolar lavage fluid, and expression of the pro-inflammatory factors in lung tissue were measured. The results revealed that HDCA administration significantly reduced MPO activity and decreased pro-inflammation as well as chemotactic cytokine generation in lung tissue (Figures 2D–2F). All findings demonstrated that HDCA attenuated organ damage and decreased mortality rate in a murine model of polymicrobial sepsis.

HDCA rescued sepsis-induced systemic immune cell hyperactivation

Systemic immune cell dysregulation, particularly the overproduction of inflammatory factors, is critical in sepsis-induced abnormalities.[3] We further analyzed how HDCA affects the systemic immune cells during sepsis by employing single-cell RNA sequencing (scRNA-seq) for peripheral blood mononuclear cells (PBMCs) of mice. After filtering the single-cell transcriptome data, a total of 26,337 high-quality cells were used for an unbiased analysis (Figure S5). As presented in Figure 3A, uniform manifold approximation and projection (UMAP) segregated PBMCs into five cell types (the clusters were conserved for a minimum of 20 cells in each sample), annotated as myeloid I cells, myeloid II cells, natural killer (NK) cells, T cells, and B cells based on their specific marker genes (Figure 3B). We found that all the cell clusters were involved in the regulation of inflammation response as revealed by the Kyoto Encyclopedia of Genes and Genomes (KEGG) pathway enrichment analysis (Figure 3C). We then extracted all gene expressions in different groups and performed gene set variation analysis (GSVA), which indicated that the cytokine-cytokine receptor interaction had the highest enrichment score in the CLP group (compared with the sham group) but remarkably decreased after HDCA treatment (Figures 3D and 3E). In particular, the cytokine profile in this signaling pathway was largely suppressed in the HDCA treatment group when compared with the CLP group (Figure 3F). Similar to the scRNA-seq results, bulk RNA-seq of peritoneal lavage fluid (PLF) cells revealed significant downregulation of the pro-inflammatory cytokine and chemokine genes when septic mice were treated with HDCA (Figure 3G). Then, we presented validation results by checking cytokine protein levels in plasma samples (Figure 3H) and inflammatory factor gene expression levels in PLF cells (Figure 3I). These results collectively suggested that HDCA can rescue the sepsis-induced overactivation of systemic immune cells.

HDCA reduced macrophage pro-inflammatory response

We next investigated the potential mechanism by which HDCA has defensive effects against polymicrobial sepsis, namely how HDCA reduces systemic inflammation. The hyperinflammation stage of sepsis is associated with enhanced immune cell activation and cytokine overexpression, which are the consequences of bacterial overload and/or elevated inflammatory signaling transduction in immune cells.[5] We hypothesized that HDCA directly impacts microbes and evaluated the anti-bacterial effects of HDCA by measuring the CFU in the blood and cecum contents. Figure S6 shows that the bacterial load in the blood and cecum contents did not exhibit a statistical shift

Figure 2. HDCA prolongs survival and alleviates acute lung injury in septic mice

(A) Kaplan-Meier survival analysis showing a 72-h survival rate of mice following surgery (n = 5–11). (B) Histological score, F4/80-positive stained cell numbers, and Ly6G-positive stained cell numbers were calculated in 10 fields per slide at 400× magnification in lung tissue (n = 5–7). (C) Representative images of the left lung labeled with hematoxylin and eosin (H&E) staining, immunohistological staining of F4/80 (macrophages, brown cell, second row), and immunohistological staining of Ly6G in lung tissue sections (neutrophils, brown cell, third row). Scale bars, 50 μm. (D) MPO activity determined in the lung tissue homogenates (n = 5–10). (E) The levels of tumor necrosis factor α (TNF-α), interleukin-1β (IL-1β), and IL-6 in bronchoalveolar lavage fluid (BALF) were determined by ELISA (n = 5–7). (F) Pro-inflammatory factor mRNA levels in the lung tissue homogenates were determined by qPCR (n = 5–7). Representative results from two independent experiments with similar results. *$p < 0.05$ (unpaired two-tailed Student's t test except for log-rank test for survival rate analysis; mean ± SEM).

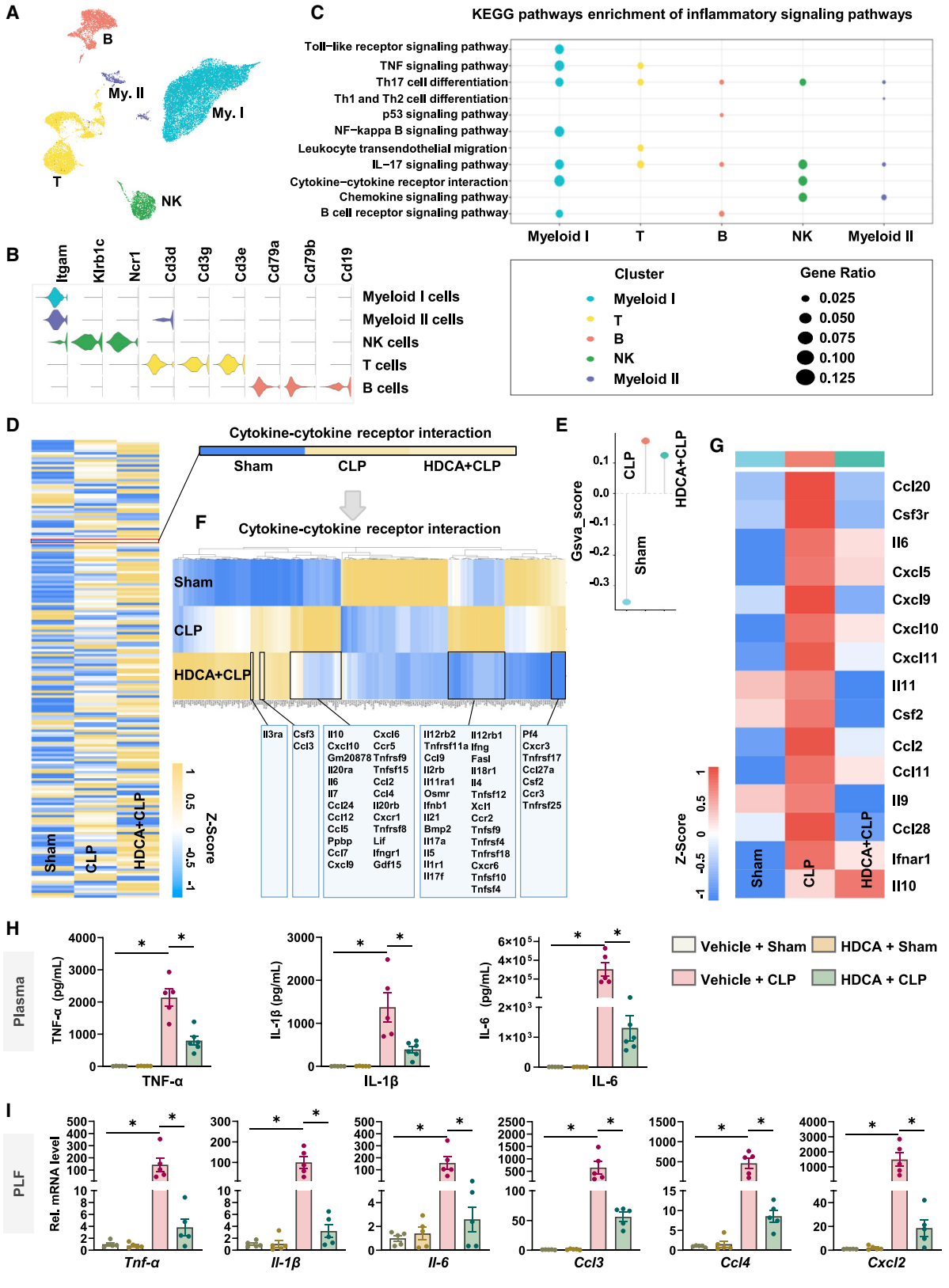

(legend on next page)

with the treatment of HDCA, which led us to investigate whether the inflammatory signaling transduction in immune cells benefits from HDCA treatment. Since macrophages and neutrophils are sentinel cells of innate immunity, which contributed to the production of early inflammatory cytokines,[5] we investigated the effects of HDCA treatment on both cells. First, we isolated peritoneal macrophages (PMs; $F4/80^{+}CD11b^{+}$cells) derived from HDCA-treated or non-treated septic mice by fluorescence-activated cell sorting to analyze their pro-inflammatory cytokine expression. We found that treatment with HDCA reduced mRNA levels of pro-inflammatory cytokines in PMs isolated from septic mice when compared with those without treatment (Figures 4A and 4B). HDCA was then tested in murine bone marrow-derived macrophages (BMDMs), human monocyte-derived macrophages (THP-1-dMs), and neutrophils for its anti-inflammatory effects. Based on the results of the CCK8 test, HDCA did not have any toxic effects on the viability of cells at the concentrations tested (ranging from 0 to 400 μM) (Figure S7). In line with *in vivo* experiments, the overexpressed pro-inflammatory factor levels in LPS-stimulated macrophages and neutrophils were remarkably reversed by HDCA treatment (Figures 4C, 4D, and S8). These results suggested that HDCA appeared to protect against sepsis by inhibiting the activation of inflammatory signaling in the immune cells.

As TLR4 signaling is a well-known signaling pathway regulating the expression of pro-inflammatory cytokines and is a key pathway in the pathophysiology of sepsis,[29] we then explored whether HDCA could inhibit TLR4 signaling, including mitogen-activated protein kinase (MAPK) and nuclear factor κB (NF-κB) in macrophages. The phosphorylation of p38, extracellular signal-regulated kinase (ERK) 1/2, and c-Jun N-terminal kinase (JNK) in the MAPK pathway, and phosphorylation of p65 in the NF-κB pathway were assessed by western blotting. As Figures 4E–4H show, the expression levels of P-P38, P-ERK, P-JNK, and P-P65 in the LPS-stimulated group were all significantly inhibited by HDCA treatment. These observations indicated that the anti-inflammatory properties of HDCA may be attributed to its inhibition of the TLR4 signaling pathway.

HDCA inhibited TLR4/MD2 complex activation

Among the key components of the inflammation process in sepsis, TLR4 plays a crucial role in the response of the cells to LPS.[30] Given that the early stimulation of TLR4 by LPS is initiated from the cell surface, we first explored whether HDCA could interfere with the binding of fluorescein isothiocyanate (FITC)-LPS to the cell surface. Macrophages (BMDM and THP-1-dMs) were co-incubated with FITC-LPS in the presence of HDCA or not for 30 min, and the fluorescence intensity of cells was analyzed by flow cytometry. We found that HDCA treatment resulted in diminished fluorescence intensity, which indicated a decreased affinity for FITC-LPS binding to membrane surface receptors (Figures 5A and 5B). If HDCA binds to LPS, it might alter the ability of LPS to bind to cell membranes. We wondered whether HDCA could bind to LPS. Surface plasmon resonance (SPR) detection of HDCA indicated that the binding ability of HDCA to LPS was extremely weak (Figure S9), suggesting that HDCA scarcely binds to LPS. Furthermore, the internalization of TLR4 receptors also inhibits the binding of FITC-LPS to the cell membrane. However, we found that the levels of TLR4 detected by anti-TLR4-PE antibodies did not differ statistically under LPS stimulation with or without HDCA (Figure S10), suggesting that HDCA did not disturb the internalization of TLR4 receptors. In addition, the expression of TLR4 and its accessory protein myeloid differentiation protein 2 (MD2) did not change in the presence of HDCA compared with the LPS group (Figure S11). The LPS-stimulated dimerization of transmembrane TLR4 in complex with MD2 and dimerization of TLR4 were responsible for inducing intracellular inflammatory signaling.[31] We then tested whether HDCA affected the dimerization of TLR4/MD2 or TLR4/TLR4. When FLAG-TLR4 and HA-MD2 plasmids were overexpressed in macrophages, HDCA pretreatment as well as co-incubation with LPS reduced the dimerization of TLR4/MD2 induced by LPS stimulation (Figures 5C and S12). Similarly, the dimerization of TLR4, which is observed after LPS treatment, can also be reduced by HDCA treatment in FLAG-TLR4 and HA-TLR4 plasmid overexpressed macrophages (Figures 5D and S12).

Meanwhile, SPR analysis was used to explore the potential interaction between HDCA and the recombinant human (rh) protein of rhTLR4/MD2 complex, rhMD2, and rhTLR4. We found that HDCA rapidly bound to the recombinant protein of rhTLR4/MD2 complex with an equilibrium dissociation constant (K_D) value of 9.91×10^{-9} M (Figure 5E), rhMD2 with a K_D value of 1.23×10^{-8} M (Figure 5F), and rhTLR4 with a K_D value of 1.29×10^{-8} M (Figure 5G) in a dose-dependent manner, suggesting an excellent binding affinity. These results revealed that HDCA may directly target the TLR4/MD2 complex.

The above results prompted us to further investigate the underlying binding mode of HDCA in the TLR4/MD2 protein by using

Figure 3. HDCA rescues sepsis-induced systemic immune cell hyperactivation

(A) UMAP visualization of cell clusters in three groups (sham, CLP, and HDCA + CLP, one mouse for each group). (B) Violin plots show the expression levels of selected marker genes across the five clusters: myeloid I cells ($Itgam^{+}$), myeloid II cells ($Itgam^{+}$), NK cells ($Klrb1c^{+}Ncr1^{+}$), T cells ($Cd3d^{+}Cd3e^{+}Cd3g^{+}$), and B cells ($Cd79a^{+}Cd79b^{+}Cd19^{+}$). (C) Scatter chart shows the enrichment results of the inflammatory pathway between CLP and HDCA + CLP groups by KEGG enrichment analysis. The different colors represent various cell types, and the points represent gene ratios. (D) GSVA analysis was calculated for each pathway based on the average expression of each gene in three group samples using the curated gene sets (C2) KEGG pathway subclass data in the molecular signatures database (MSigDB) (yellow, upregulated; blue, downregulated). (E) Cleveland's dot plot shows the GSVA score of the cytokine-cytokine receptor interaction of each group. (F) Heatmap shows the *Z* score of gene expression from cytokine-cytokine receptor interaction. (G) Heatmap shows the mean expression of 15 cytokines and chemokines in PLF cells. Colored bars indicate the expression levels (red, upregulated; blue, downregulated). Rows represent cytokine/chemokines and columns represent groups (n = 5). (H) The protein levels of TNF-α, IL-1β, and IL-6 in mouse plasma were determined by ELISA (n = 5–6). (I) Pro-inflammatory factor mRNA levels of PLF were analyzed by qPCR (n = 5). Representative results from two independent experiments with similar results (H and I). *$p < 0.05$ (one-way ANOVA with Bonferroni's post hoc tests in H and I; mean ± SEM).

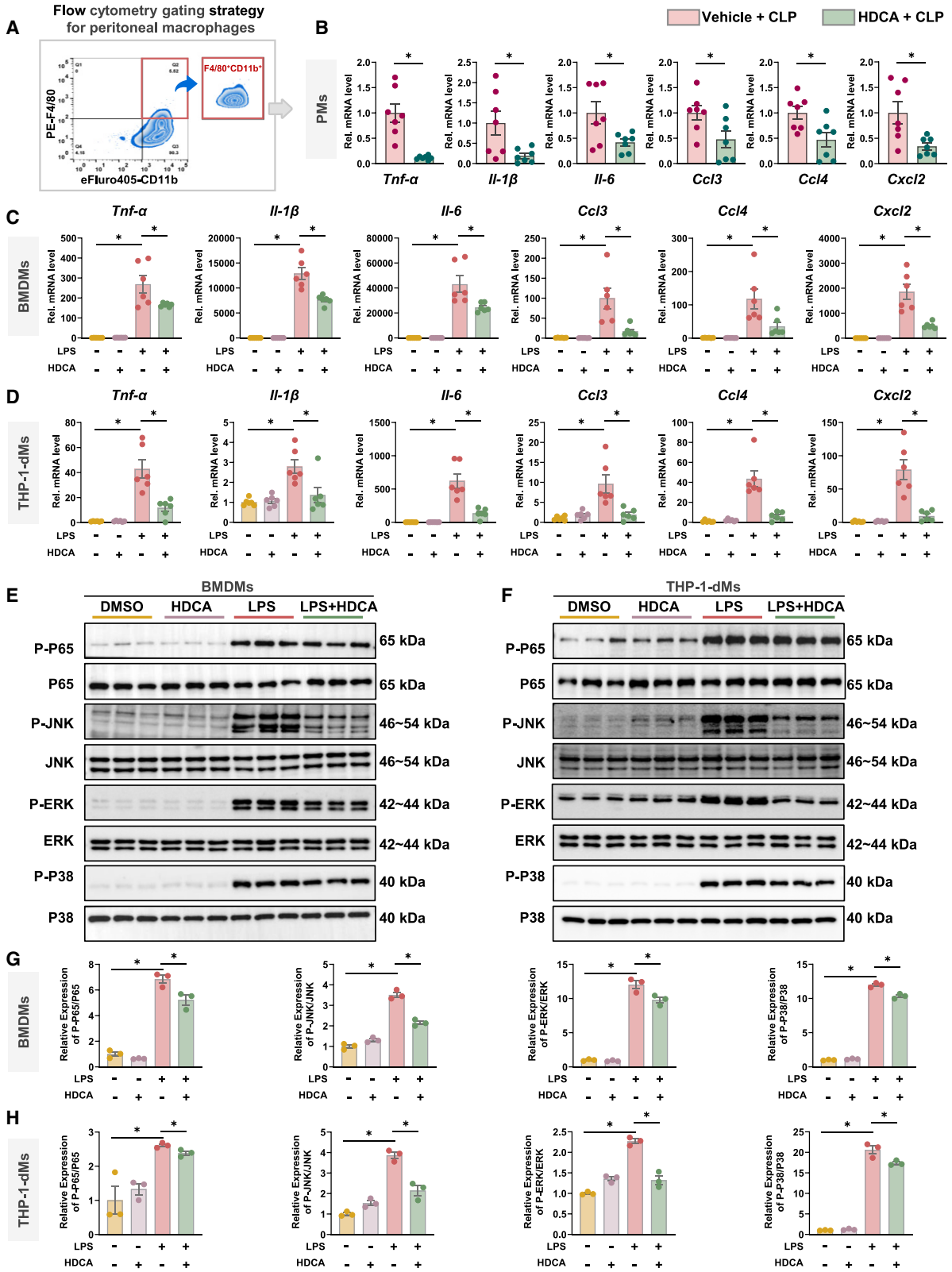

(legend on next page)

molecular simulation of the LPS/TLR4/MD2 complex (PDB: 3FXI). HDCA was shown to reside buried within the binding pocket and to overlap in some capacity with the binding sites of LPS (docking score of −3.332), which suggests a competitive inhibition mechanism of LPS by HDCA (Figure 5H). Based on computer simulations, three amino acid residues are most likely to form hydrogen bonds with HDCA: Ser^{120}, Asp^{294}, and Lys^{362} (Figure 5I). To provide a qualitative assessment of the key residues with the most contributions in HDCA binding to rhTLR4/MD2, three new protein mutations, $rhMD2^{S120A}$, $rhTLR4^{D294A}$, and $rhTLR4^{K362A}$, were prepared. As determined by the SPR assay, HDCA exhibits a much lower binding affinity to these three mutations than wild-type HDCA: $rhMD2^{S120A}$ with a K_D value of 2.33×10^{-7} M (Figure 5J), $rhTLR4^{D294A}$ with a K_D value of 2.44×10^{-3} M (Figure 5K), and $rhTLR4^{K362A}$ with a K_D value of 2.49×10^{-5} M (Figure 5L), demonstrating that HDCA may interact with multiple amino acid residues of TLR4/MD2 complex, including Ser^{120} of MD2 and Lys^{362}, Asp^{294} of TLR4. Together, our results demonstrate that HDCA disrupts LPS interaction with the TLR4/MD2 complex and elucidate the possible mechanism of HDCA binding to the rhTLR4/MD2 protein pocket, suggesting HDCA as an endogenous inhibitor of the TLR4 receptor.

TLR4 signaling is required for HDCA's anti-inflammatory effects in sepsis

TLR4 knockout ($TLR4^{-/-}$) mice (Figure S13A) were used to further confirm the underlying mechanisms that drive the anti-inflammatory properties of HDCA. Given that TLR4 signaling is essential for the maintenance of inflammation during sepsis,[32] we first assessed the inflammation levels in $TLR4^{-/-}$ mice subjected to CLP surgery. Despite the lower level of inflammatory factors in $TLR4^{-/-}$ mice than in wild-type mice, mRNA levels of inflammatory factors in PLF and lung tissue revealed an enhanced pro-inflammatory response in $TLR4^{-/-}$ septic mice compared with sham-operated $TLR4^{-/-}$ mice (Figures S13B and S13C), indicating that TLR4-independent signaling pathways also mediated the sepsis-associated pro-inflammatory response in $TLR4^{-/-}$ mice. Pathological evaluation revealed more severe structural damage in the alveoli, accompanied by congestion, collapse, and thickened alveolar wall in CLP-operated $TLR4^{-/-}$ mice compared with sham-operated $TLR4^{-/-}$ mice. Meanwhile, more $F4/80^+$ macrophages and $Ly6G^+$ neutrophils were detected in the CLP group than in the sham group. However, the histopathological damage and inflammatory cell infiltration was not relieved in the HDCA-treated group compared with the CLP group (Figures 6A and 6B). In addition, the inflammatory cytokine levels in plasma, lung tissue, and PLF were not attenuated by HDCA treatment in $TLR4^{-/-}$ septic mice (Figures 6C–6E). *In vitro*, the phosphorylation of P-P65, P-JNK, P-ERK, and P-P38, or the expression of pro-inflammatory cytokines, did not relieve the HDCA-treated $TLR4^{-/-}$ BMDMs (Figure S14). Taken together, these data suggested that the protective effect of HDCA against sepsis may be, at least in part, due to the inhibition of the TLR4 signaling pathway.

DISCUSSION

In this study we confirmed HDCA as an endogenous TLR4 inhibitor, which inhibits systemic inflammation, reduces organ damage, and prolongs survival time in septic mice. Mechanistically, HDCA inhibits the formation of LPS/TLR4/MD2 ternary complexes and blocks the activation of TLR4 downstream signaling pathways in macrophages. Thus, our study provided evidence for the design of effective treatment strategies to alleviate sepsis and broadened our understanding of the host-gut microbiome relationship in sepsis.

HDCA species include HDCA, taurohyodeoxycholic acid (THDCA), and glycohyodeoxycholic acid (GHDCA). Compared with the serum/plasma levels of THDCA and GHDCA (0%–1%), HDCA is more abundant in mice and humans.[33,34] Although the natural abundance of HDCA is lower in human plasma than in rodents,[34] pharmacological levels of HDCA, if administered, would be achievable for a favorable therapeutic response. Moreover, the feature of the delayed release of bile acids from the intestine into the blood circulatory system through enterohepatic reabsorption might allow HDCA to achieve prolonged effects on target cells. It is currently recognized that HDCA is mainly generated from gut microbiota; however, the biosynthesis of HDCA is different among mammalian species. In rats, HDCA was derived from muricholic acid via a strain of *Eubacterium* (EMBL: AJ238611)[25] or from lithocholic acid (LCA) by cytochrome P450 3A4 (CYP3A4).[35,36] Our study has supported the notion that HDCA may be derived from *Eubacterium*, as we found that the relative abundance of the taxa *Eubacterium_R* was positively correlated with cecal HDCA levels, while supplementation of an available strain of *Eubacterium* can significantly increase the level of HDCA in feces. However, no species-level annotation could be assigned to EMBL: AJ238611 with the current genome annotation in the microbial database. Therefore, further clarification of specific HDCA-producing bacteria in mice relies on the development of an enhanced functionally and taxonomically annotated bacterial gene catalog. In humans, HDCA is presumably derived from

Figure 4. HDCA reduces macrophage pro-inflammatory response and inhibits the TLR4 signaling pathway

(A) Flow cytometry gating strategy for sorting PMs ($F4/80^+CD11b^+$) in PLF. (B) Pro-inflammatory factor mRNA levels in PMs ($F4/80^+CD11b^+$) at 12 h after CLP surgery were determined by qPCR (n = 7). (C) Pro-inflammatory factor mRNA levels in BMDMs after LPS (100 ng/mL) stimulated for 6 h were determined by qPCR (n = 6). (D) Pro-inflammatory factor mRNA levels in THP-1-dMs after LPS (500 ng/mL) stimulated for 6 h were determined by qPCR (n = 6). (E) Protein expression of phosphorylated P65, JNK, ERK, and P38 (P-P65, P-JNK, P-ERK, P-P38), and total P65, P38, ERK, and JNK in BMDMs after LPS (100 ng/mL) stimulation for 15 min with or without 20 μM HDCA by immunoblotting analysis. (F) Protein expression of P-P65, P-JNK, P-ERK, and P-P38, and total P65, P38, ERK, and JNK in THP-1-dMs after LPS (500 ng/mL) stimulation for 15 min with or without 20 μM HDCA by immunoblotting analysis. (G) Phosphorylated levels were normalized to total proteins in BMDMs (n = 3). (H) Phosphorylated levels were normalized to total proteins in THP-1-dMs (n = 3). Representative results from two (B) or three (C–H) independent experiments with similar results. *$p < 0.05$; ns, not significant (unpaired two-tailed Student's t test in B; one-way ANOVA with Bonferroni's post hoc tests in C, D, G, and H; mean ± SEM).

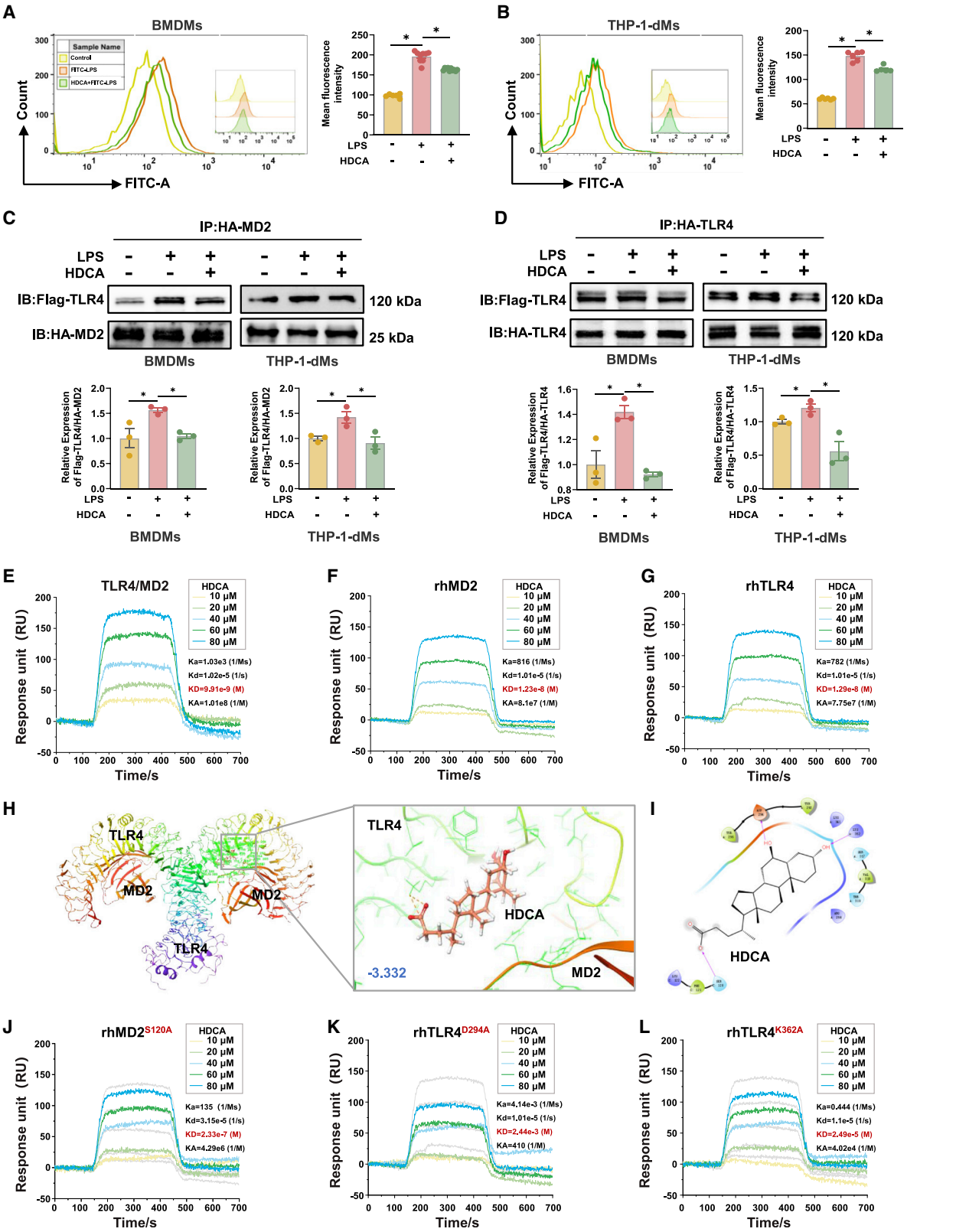

(legend on next page)

taurolithocholic acid and LCA through the CYP3A4-mediated 6α-hydroxylation pathway.[37,38] It is not clear whether or not *Eubacterium*, the second most common bacterial genus found in the human intestine (after the *Bacteroides*),[39] is involved in the synthesis of HDCA. Interestingly, the concentration of HDCA in mouse feces was significantly increased after oral inoculation with *E. limosum*, which was isolated from human intestine. This result suggests that *Eubacterium* may also be a contributor to endogenous HDCA in humans. In addition, other reports indicated that the fecal levels of HDCA in pigs are associated with *Clostridium* and *Parabacteroides*.[40] However, this was not observed in our study, suggesting that the bacterial strains associated with HDCA levels may be heterogeneous in different diseases and hosts. Currently, the reason for HDCA reduction in sepsis is not clear. We speculate that the reduction of HDCA in sepsis may result from two aspects. (1) The lower levels of HDCA are associated with lower relative abundances of gut microbes involved in HDCA production. Our results from metagenomic sequencing analysis showed that the relative abundance of the genus *Eubacterium*, which has been reported to be one of the gut microbiota that produces HDCA *in vitro*, was remarkably decreased in the cecal content samples of septic mice (Figure 1H). (2) A loss of homeostasis of bile acid is associated with sepsis, as LPS-mediated inflammation causes hepatocytes to degrade their transporters,[41] thus leading to dysregulation of secondary bile acid levels.

Tissue macrophages, as known, are highly plastic cells that can be classified into two types: pro-inflammatory M1 macrophages and anti-inflammatory M2 macrophages.[42] To further clarify whether the anti-inflammatory effect of HDCA is associated with M2, we assessed the phenotype of PMs ($F4/80^{+}CD11b^{+}$) in CLP and HDCA + CLP mice by quantifying the cell surface expression of inducible nitric oxide synthase (M1 macrophage marker) and CD206 (M2 macrophage marker) by flow cytometry. Figure S15 shows that HDCA treatment significantly reduced the M1 macrophage percentage, while a higher percentage of M2 macrophages was evident in HDCA-treated mice compared with the CLP group. In light of these findings, the anti-inflammatory effect of HDCA may be associated with the promotion of macrophage polarization, but how HDCA regulates macrophage polarization requires further investigation.

As polymicrobial sepsis is expected to activate multiple TLR signaling pathways in response to microbial infection, we further tested whether HDCA has an anti-inflammatory effect on other TLR agonists. We examined cytokine expression after treatment with the specific TLR agonists for 6 h, including Cu-CPT22 (for TLR1/2), FEL-1 (for TLR2/6), LPS (for TLR4), poly I:C (for TLR3), R848 (for TLR7/8), and imiquimod (for TLR7). We found that HDCA potently inhibited the expression of inflammatory cytokines induced by TLR4 and TLR3 receptors, whereas this agent showed a limited effect on the rest of the receptors (Figure S16). In contrast to TLR4, TLR3 may contribute less to macrophage inflammation, as evidenced by much less expression of cytokines; therefore, TLR4 activation is still the main target of HDCA during inflammation. However, future work may still focus on the modulation between TLR3 and sepsis, and whether HDCA participates in the regulatory process.

Our results have provided solid evidence that HDCA is a natural TLR4 antagonist, which inhibits TLR4 activation and TRL4 downstream signaling by competitively binding to LPS in macrophages. Excessive activation of TLR4 signaling is a distinct immunological phenotype in immune disorders, including sepsis, drug addiction, neuropathic pain, and autoimmune diseases.[43–46] It appears that the therapeutic potential of HDCA is associated with various TLR4 overactivated diseases. Studies on HDCA metabolism in humans have shown that oral administration of HDCA exhibited insignificant toxic transformation in the body.[47] However, further studies with additional pre-clinical models are needed to gain a more comprehensive understanding of the effect of HDCA on inflammatory diseases. Indeed, naturally occurring HDCA generally does not exert the most effective anti-inflammatory activities.[48] Thus, further structural modification of HDCA to enhance its druggability may hold the potential to generate anti-inflammatory agents more potent than HDCA itself.

Overall, our results have provided supporting evidence that HDCA as a potential endogenous TLR4 inhibitor could protect against the development of sepsis in the mouse model and has the potential to be used as a treatment for sepsis as well as other inflammatory disorders involving TLR4 signaling.

Figure 5. Identification of TLR4/MD2 as the molecular target of HDCA

(A) BMDMs were incubated with 100 μg/mL FITC-LPS in the absence or presence of 10 μM HDCA for 30 min. The binding of FITC-LPS was analyzed by flow cytometry after washing. The binding of FITC-LPS was expressed as mean fluorescence intensity (MFI) (n = 6–10). (B) THP-1-dMs were incubated with 100 μg/mL FITC-LPS in the absence or presence of 20 μM HDCA for 30 min. The binding of FITC-LPS was analyzed by flow cytometry after washing. The binding of FITC-LPS was expressed as MFI (n = 5–6). (C) Dimerization of TLR4/MD2 was detected after being pre-treated with or without HDCA for 1 h followed by LPS stimulation for 30 min in BMDMs and THP-1-dMs transfected with FLAG-TLR4 and HA-MD2 plasmids. These cells were lysed and subjected to SDS-PAGE after immunoprecipitation with an anti-HA antibody. Statistical data are from three independent experiments. (D) Dimerization of TLR4/TLR4 was assessed after being pre-treated with or without HDCA for 1 h followed by LPS stimulation for 30 min in BMDMs and THP-1-dMs transfected with FLAG-TLR4 and HA-TLR4 plasmids. These cells were lysed and subjected to SDS-PAGE after immunoprecipitation with an anti-HA antibody. Statistical data are from three independent experiments. (E–G) SPR analysis of HDCA (10, 20, 40, 60, and 80 μM) binding to the recombinant (E) rhTLR4/MD2 complex protein, (F) rhMD2 protein, and (G) rhTLR4 protein. (H) Molecular docking analysis of HDCA with the TLR4/MD2 complex. (I) Binding sites between HDCA and TLR4/MD2 complex. (J–L) SPR analysis of HDCA (10, 20, 40, 60, and 80 μM) binding to the recombinant (J) $rhMD2^{S120A}$ protein, (K) $rhTLR4^{D294A}$ protein, and (L) $rhTLR4^{K362A}$ protein. The gray curve represents the response curve of wild-type recombinant protein. Representative results from two (A and B) or three (C–G, J–L) independent experiments with similar results. *$p < 0.05$ (one-way ANOVA with Bonferroni's post hoc tests in A–D; mean ± SEM).

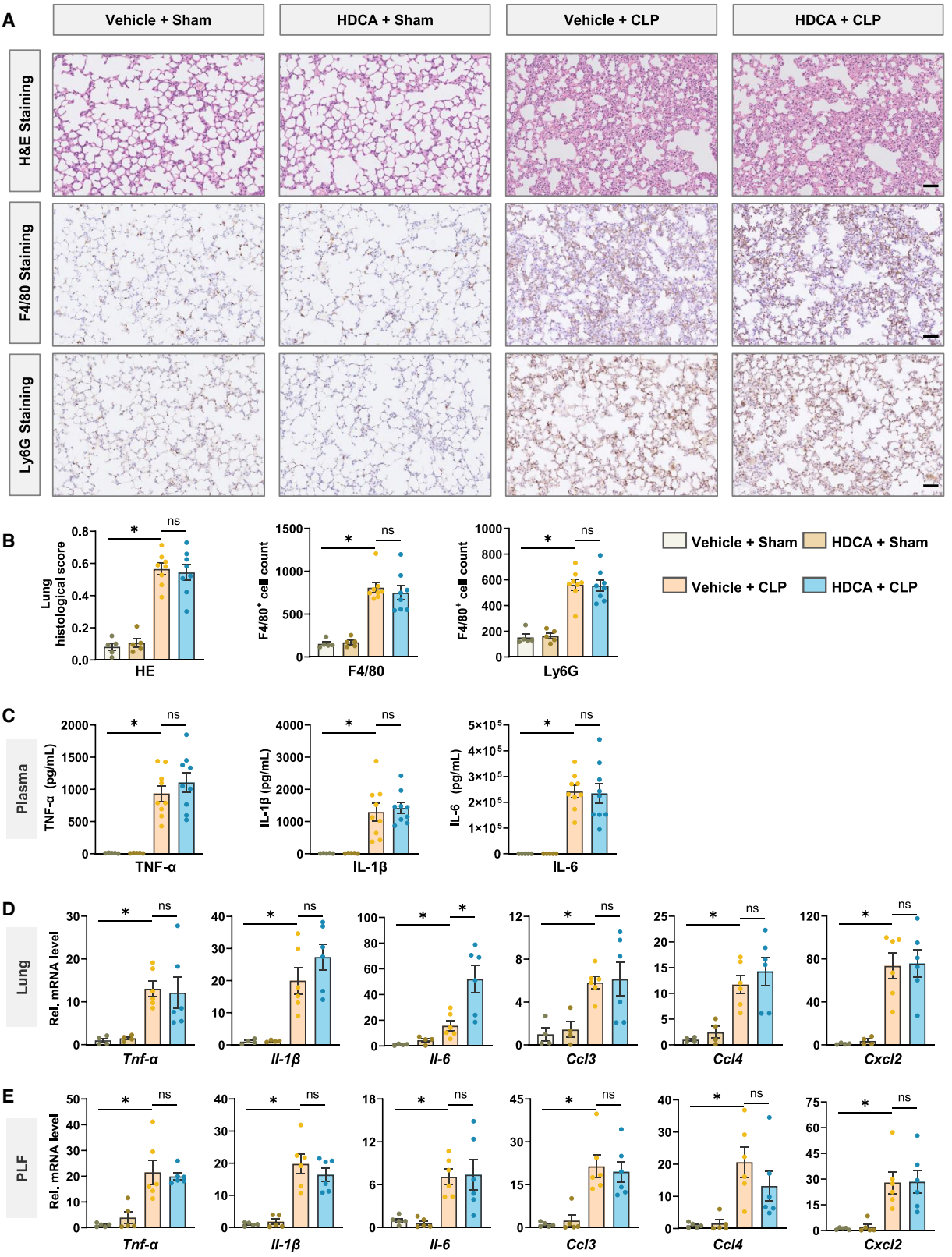

(legend on next page)

MATERIALS AND METHODS

Human study

The Medical Ethics Committee of Southern Medical University approved all experiments that were conducted on humans in accordance with the Declaration of Helsinki, which is the ethical code adopted by the World Medical Association (approval number NFEC-2021-139). Prior to inclusion, all participants signed an informed consent form. The inclusion criteria of sepsis were defined as follows: (1) diagnosed within 24 h of intensive care unit admission based on Sepsis 3.0 criteria;[49] (2) aged 18–80 years. The exclusion criteria were patients: (1) with pregnancy or perinatal complications; (2) who received HDCA-containing drugs (e.g., bezoar); (3) with missing laboratory or clinical data. After recruitment, all clinical features of sepsis patients were recorded. We enrolled 47 sepsis patients and 13 healthy control subjects matched for age and gender (clinical indices are shown in Table S1).

Experimental animals

Male C57BL/6J wild-type mice and TLR4$^{-/-}$ mice at 6–8 weeks old were purchased from GemPharmatech (Nanjing, China). All procedures involving animals were approved by the Animal Care and Use Committee of Southern Medical University (Guangzhou, China) with approval number SMUL2021094. The severe polymicrobial sepsis model was performed by CLP. After anesthetizing the mice, the cecum was exposed through a midline incision. A through-and-through puncture was made into the cecum using an 18-gauge needle after it had been isolated and ligated with a 4-0 surgical suture. The cecum was reset and sutured after a portion of cecal contents was extruded. Sham-operated mice underwent laparotomy without ligation and puncture. All mice were resuscitated with 1 mL of prewarmed normal saline. Mice were sacrificed 12 h after surgery to examine systemic inflammation and organ damage, and survival rate was recorded for 72 h. A 20 mg/kg dose of HDCA (Aladdin, China) was administered to mice by oral gavage 2 h before the CLP operation. Control mice received the equivalent volume of 0.5% carboxymethylcellulose sodium (CMC-Na). The gut microbiota of mice was depleted by administering an antibiotic cocktail (100 mg/kg vancomycin, 200 mg/kg neomycin sulfate, metronidazole, and ampicillin) intragastrically for 3 days. *E. limosum* was orally administered to mice for 7 days before CLP, and its anti-inflammatory effects and organ protection were evaluated at 12 h after surgery to explore its role in polymicrobial sepsis.

Sorting, isolation, and culture of cells

Sorting of PMs (F4/80^{+}CD11b^{+}) was performed using the Beckman Coulter MoFlo XDP after peritoneal cells were stained with antibodies against euro-405-CD11b (#48-0112-82, eBioscience, Invitrogen) and PE-F4/80 (#12-4801-82, eBioscience, Invitrogen). BMDMs were isolated from mouse tibia and femurs. Cells were matured in Dulbecco's modified Eagle's medium containing 1% penicillin-streptomycin, 10% fetal bovine serum (FBS), and 20 ng/mL macrophage colony stimulating factor (#416-ML-050, R&D Systems, USA) for 7 days. THP-1 cells (ATCC TIB-202) were cultured in 1640 medium supplemented with 1% penicillin and 10% FBS streptomycin and then differentiated into macrophages (THP-1-dMs) by stimulation with phorbol 12-myristate 13-acetate (5 ng/mL, #S7791, Selleck, China) for 48 h.

Quantitative analysis of HDCA

A liquid chromatography-tandem mass spectrometry system (LC-MS/MS) was used for quantitative analysis of HDCA. The cecal content sample was ground down to homogeneity by adding ultrapure water proportionally (g/mL = 1:9) upon precise weighing.

The plasma sample was collected from the hepatic portal vein of mice. Methanol (1:4, v/v) was used to precipitate proteins from 300 μL of homogeneous cecal content or 100 μL of plasma. After centrifuging at 13,000 rpm and 4°C for 15 min, the supernatant was collected and dried with nitrogen. Insoluble impurities were removed after resuspension in 100 μL of methanol and centrifugation for 10 min at 13,000 rpm and 4°C. Analysis was conducted with a TSQ Vantage triple quadrupole mass spectrometer and Prelude SPLC system from Thermo Fisher Scientific. A Hypersil Gold C^{18} column (1.9 μm, 100 mm × 2.1 mm) was used with isocratic elution (solvent composition: A solution, 5 mM ammonium acetate and 0.1% [v/v] formic acid; B solution, methanol) as mobile phase. A temperature of 40°C was set for the column. TraceFinder software (version 3.3 sp1, Thermo Fisher Scientific, USA) was used for data acquisition and processing.

Metagenomic sequencing analysis of mouse cecal contents

The cecal contents of the mice (n = 8 from sham-operated and n = 8 CLP surgery mice) were collected and sent to BGI-Shenzhen (China) for metagenomic analysis. Genomic DNA from feces was extracted, quantified, and checked for preparation of DNA libraries. Library construction and DNA sequencing were performed on the BGISEQ-500 platform as previously described.[50] Data were cleaned using SOAPnuke v.1.5.2,[51] and high-quality reads were assembled by Megahit software.[52] Kraken2[53] was used for taxonomy annotation, species abundance analysis, and comparison of metagenomic data between different samples. A Wilcoxon rank-sum test was performed to measure the diversity of the microbial alpha diversity, and the PERMANOVA test was performed for beta diversity.

Figure 6. TLR4$^{-/-}$ abolished the protective effect of HDCA in septic mice

(A) Representative images of the left lung labeled with H&E staining, immunohistological staining of F4/80 (macrophages, brown cell, second row), and immunohistological staining of Ly6G in lung tissue sections (neutrophils, brown cell, third row). Scale bars, 50 μm. (B) Histological score, F4/80-positive stained cell numbers, and Ly6G-positive stained cell numbers were calculated in 10 fields per slide at 400× magnification in lung tissue (n = 5–8). (C) The levels of TNF-α, IL-1β, and IL-6 in mouse plasma were determined by ELISA (n = 5–9). (D) Pro-inflammatory factor mRNA levels in the lung tissue homogenates were determined by qPCR (n = 4–6). (E) Pro-inflammatory factor mRNA levels in PLF were determined by qPCR (n = 5–6). Representative results from three independent experiments with similar results. ns, not significant (one-way ANOVA with Bonferroni's post hoc tests; mean ± SEM).

Single-cell RNA sequencing and data processing

PBMCs were isolated from the inferior vena cava of mice (sham, CLP, and HDCA + CLP, n = 1) and performed according to the manufacturer's protocol (#P6340, Solarbio, China). The cell viability of each sample exceeds 90%. The GemCode Single Cell platform (10x Genomics) was used to determine the transcriptome of single cells, and the operating procedure is based on standard manufacturer's instructions as described previously.[54] Transcriptome data were demultiplexed and mapped to the mm39 transcriptome with Cell Ranger Software Suite 5.0.1.[55] The Seurat package 4.0.6[56] was used for integration in R 4.0.3 after obtaining the expression matrix for each sample. From this, all cells were removed that had more than 5,000 or fewer than 200 expression genes, over 30,000 unique molecular identifiers, over 15% derived from mitochondrial genes, over 50% derived from the ribosome genome, or over 0.01% derived from the hemoglobin genome. Doublet cell and cell-free mRNA were also removed.[57,58] A normalization function within the Seurat package was used to normalize the expression matrices of the remaining 26,337 cells. With the default settings in the RunUMAP function, the first five principal components were further summarized using UMAP dimensionality reduction. With the help of canonical marker genes, cell clusters within the resulting two-dimensional representation were annotated to known biological cell types. Different periods were extracted, and KEGG enrichment analysis was performed using the cluster profile package 3.18.1.[59] The GSVA package 1.42.0[60] was used to analyze the KEGG subset of canonical pathways described in curated gene sets contained in the molecular signature database.

Transcriptome analysis of mice peritoneal lavage

Peritoneal lavage solution from mice (n = 5 in sham, n = 5 in CLP, and n = 5 in HDCA + CLP) was centrifuged at 1,000 rpm and 4°C for 10 min. The total RNA samples were extracted by the TRIzol method for quantitative and quality inspection. Library preparation, establishment, and sequencing were performed on the Illumina Novaseq 6000 platform (Novogene Bioinformatics Technology, Beijing, China). Gene expression levels were obtained by aligning with the mm39 reference genome and further converted into trusted platform module values for subsequent analysis. The average expression levels of inflammatory factors and cytokines with different group characteristics were extracted, and heatmaps were drawn and displayed using the heatmap package 1.0.12.

Flow-cytometry analysis of LPS-binding assay

BMDMs or THP-1-dMs (1×10^6) were collected and co-incubated with FITC-LPS (100 μg/mL, #F8666, Sigma, St. Louis, MO) with or without HDCA (10 μM HDCA in BMDMs, 20 μM HDCA in THP-1-dMs) for 30 min at room temperature. The cells were washed three times to remove unbound FITC-LPS and resuspended in cell staining buffer (#420201, BD, China) for analysis. The binding of FITC-LPS was determined by flow cytometry using a FACSCalibur apparatus (BD Bioscience, Bedford, MA, USA). The mean fluorescence intensity was analyzed using FlowJo software (v.10, Tree Star, USA).

SPR experiment

An SPR experiment was conducted to determine HDCA binding affinity to recombinant proteins, including rhTLR4 (#10146-H08B, Sino Biological, China), rhMD2 (#MB16MY1221, Sino Biological), $rhTLR4^{D294A}$ (#MF16JU2051, Sino Biological), $rhTLR4^{K362A}$ (#MF16JU1442, Sino Biological), $rhMD2^{S120A}$ (#MB16MY2092, Sino Biological), and TLR4/MD2 complex protein (#3146-TM-050, R&D Systems, USA). Three microliters of 0.3 mg/mL recombinant protein was immobilized on the protein chip and activated with 10 mM $NiSO_4$. The different concentrations of HDCA (at 10, 20, 40, 60, and 80 μM) were diluted with Dulbecco's PBS (DPBS) and flowed in the mobile phases at a rate of 30 μm/min. The binding signal was recorded by PlexArray HT specialized software (Plexera Bioscience, USA). Data were analyzed using Origin 9.0 (OriginLab, USA) and BIAevaluation 4.1.1.

Immunoprecipitation

Human and murine overexpression wild-type and mutant plasmids were purchased from Gikai Gene (Genechem, Shanghai, China). The Endotoxin-Free Plasmid Extraction Kit (#D6950-01B, Omega) was used to extract the plasmid. After transfection for 48 h, BMDMs and THP-1-dMs were pre-treated with HDCA for 1 h and then stimulated with LPS for 30 min, or HDCA and LPS were co-intubated for 30 min in a cell-culture chamber (10 μM HDCA and 100 ng/mL LPS in BMDMs, 20 μM HDCA and 500 ng/mL LPS in THP-1-dMs). Immunoprecipitation was conducted following the instructions of the Pierce Classic IP Kit (#26146, Thermo Fisher Scientific). In brief, cells were washed once with DPBS to remove any remaining residuals. Immunoprecipitation lysate was added to enable cracking for 10 min and centrifuged at 12,000 × *g* for 15 min. The cell lysis supernatant was collected and incubated overnight with HA antibody (1:100, #51064-2-AP, Proteintech, China) at 4°C. The next day, the protein A/G beads were added to the supernatant and incubated at room temperature for 1 h. After washing the beads with cold lysis buffer three times, beads were resuspended in 1× SDS sample buffer and boiled at 100°C for 5 min, followed by a western blot assay.

Simulations of HDCA docking with TLR4/MD2

The docking server Schrodinger-Maestro (version 11.1) was used to predict and assess interactions between the HDCA (structure obtained from PubChem) and humanTLR4/MD2 complex (obtained from the Protein Data Bank, PDB: 3FXI). The ligands and water molecules that are not involved in docking were removed from the protein structure, after which polar hydrogen atoms and charges were added.[61,62] Receptor grid generation was used to choose a grid box that enclosed the whole LPS-binding site. Docking was conducted when HDCA was docked into the grid box (LPS-binding site). Other parameters were set as default during the docking. The docking images and docking scores were exported to be evaluated.

Statistical analysis

Statistics and mapping were performed by GraphPad Prism 9. A two-tailed, unpaired Student's t test was used for determining the

statistical difference between two groups, and one-way ANOVA with Bonferroni's multiple comparisons test was used for more than two groups. The log-rank statistics were used to evaluate the survival curves of septic mice. Spearman's rank correlation test was used to analyze the correlation. All experimental results are expressed as mean ± standard error of mean (SEM). A p value of <0.05 is considered significant, and the statistical sample size (n) is listed in each figure legend.

DATA AVAILABILITY

Metagenomic sequencing data and transcriptome data are available in the SRA database: Bioproject PRJNA859637 and PRJNA802966. Genomic scRNA-seq data are available at the GEO database: GSE195965. Raw data not included therein can be obtained from the corresponding authors upon reasonable request.

SUPPLEMENTAL INFORMATION

Supplemental information can be found online at https://doi.org/10.1016/j.ymthe.2023.01.018.

ACKNOWLEDGMENTS

We thank Critical Care Medicine of Southern Medical University Nanfang Hospital for its help. This study was supported by the National Key R&D Program of China (2022YFA0806400), the National Natural Science Foundation of China (81873926, 32071124, 82130063, and 81871604), Special Support Plan for Outstanding Talents of Guangdong Province (2019JC05Y340), and Natural Science Foundation of Guangdong Province (2017A030313590).

AUTHOR CONTRIBUTIONS

Y.J., Z.C., W.J., and P.C. designed the study, interpreted the data, drafted and edited the manuscript, and supervised the study. J.L., R. Li, and P.C. prepared all of the figures and wrote the manuscript. J.L., Y.C., R. Li, T.C., F.M., R. Liu, M.C., R.W., and Z.C. performed the experiments and analyzed the data. X.Z. and Z.W. participated in the bioinformatics analysis. Y.G. and H.H. analyzed the clinical data. H.F. was responsible for the bacteria culture. Z.Z., Y.D., H.L., S.H., S.C., F.W., N.S., Y.Z., and M.X. collected the clinical samples.

DECLARATION OF INTERESTS

The authors declare no competing interests.

REFERENCES

1. Rudd, K.E., Johnson, S.C., Agesa, K.M., Shackelford, K.A., Tsoi, D., Kievlan, D.R., Colombara, D.V., Ikuta, K.S., Kissoon, N., Finfer, S., et al. (2020). Global, regional, and national sepsis incidence and mortality, 1990-2017: analysis for the Global Burden of Disease Study. Lancet (London, England) *395*, 200–211.
2. Fleischmann-Struzek, C., Mellhammar, L., Rose, N., Cassini, A., Rudd, K.E., Schlattmann, P., Allegranzi, B., and Reinhart, K. (2020). Incidence and mortality of hospital- and ICU-treated sepsis: results from an updated and expanded systematic review and meta-analysis. Intensive Care Med. *46*, 1552–1562.
3. Bosmann, M., and Ward, P.A. (2013). The inflammatory response in sepsis. Trends Immunol. *34*, 129–136.
4. Delano, M.J., and Ward, P.A. (2016). The immune system's role in sepsis progression, resolution, and long-term outcome. Immunol. Rev. *274*, 330–353.
5. van der Poll, T., Shankar-Hari, M., and Wiersinga, W.J. (2021). The immunology of sepsis. Immunity *54*, 2450–2464.
6. Rooks, M.G., and Garrett, W.S. (2016). Gut microbiota, metabolites and host immunity. Nat. Rev. Immunol. *16*, 341–352.
7. Beyaert, R., and Libert, C. (2018). How good roommates can protect against microbial sepsis. Cell Host Microbe *23*, 283–285.
8. Haak, B.W., Prescott, H.C., and Wiersinga, W.J. (2018). Therapeutic potential of the gut microbiota in the prevention and treatment of sepsis. Front. Immunol. *9*, 2042.
9. Adelman, M.W., Woodworth, M.H., Langelier, C., Busch, L.M., Kempker, J.A., Kraft, C.S., and Martin, G.S. (2020). The gut microbiome's role in the development, maintenance, and outcomes of sepsis. Crit. Care *24*, 278.
10. Niu, M., and Chen, P. (2021). Crosstalk between Gut Microbiota and Sepsis*9* (Burns & trauma), p. tkab036.
11. Kullberg, R.F.J., Wiersinga, W.J., and Haak, B.W. (2021). Gut microbiota and sepsis: from pathogenesis to novel treatments. Curr. Opin. Gastroenterol. *37*, 578–585.
12. Krautkramer, K.A., Fan, J., and Bäckhed, F. (2021). Gut microbial metabolites as multi-kingdom intermediates. Nat. Rev. Microbiol. *19*, 77–94.
13. Wei, Y., Gao, J., Kou, Y., Liu, M., Meng, L., Zheng, X., Xu, S., Liang, M., Sun, H., Liu, Z., and Wang, Y. (2020). The intestinal microbial metabolite desaminotyrosine is an anti-inflammatory molecule that modulates local and systemic immune homeostasis. FASEB J. : official Publ. Fed. Am. Societies Exp. Biol. *34*, 16117–16128.
14. Parada Venegas, D., De la Fuente, M.K., Landskron, G., González, M.J., Quera, R., Dijkstra, G., Harmsen, H.J.M., Faber, K.N., and Hermoso, M.A. (2019). Short chain fatty acids (SCFAs)-Mediated gut epithelial and immune regulation and its relevance for inflammatory bowel diseases. Front. Immunol. *10*, 277.
15. Gong, S., Yan, Z., Liu, Z., Niu, M., Fang, H., Li, N., Huang, C., Li, L., Chen, G., Luo, H., et al. (2019). Intestinal microbiota mediates the susceptibility to polymicrobial sepsis-induced liver injury by granisetron generation in mice. Hepatology *69*, 1751–1767.
16. Zhang, H., Xu, J., Wu, Q., Fang, H., Shao, X., Ouyang, X., He, Z., Deng, Y., and Chen, C. (2022). Gut microbiota mediates the susceptibility of mice to sepsis-associated encephalopathy by butyric acid. J. Inflamm. Res. *15*, 2103–2119.
17. Schwarzenberg, S.J., and Bundy, M. (1994). Ursodeoxycholic acid modifies gut-derived endotoxemia in neonatal rats. Pediatr. Res. *35*, 214–217.
18. Chang, S., Kim, Y.H., Kim, Y.J., Kim, Y.W., Moon, S., Lee, Y.Y., Jung, J.S., Kim, Y., Jung, H.E., Kim, T.J., et al. (2018). Taurodeoxycholate increases the number of myeloid-derived suppressor cells that ameliorate sepsis in mice. Front. Immunol. *9*, 1984.
19. Wahlström, A., Sayin, S.I., Marschall, H.U., and Bäckhed, F. (2016). Intestinal crosstalk between bile acids and microbiota and its impact on host metabolism. Cell Metab. *24*, 41–50.
20. Zheng, X., Chen, T., Jiang, R., Zhao, A., Wu, Q., Kuang, J., Sun, D., Ren, Z., Li, M., Zhao, M., et al. (2021). Hyocholic acid species improve glucose homeostasis through a distinct TGR5 and FXR signaling mechanism. Cell Metab. *33*, 791–803.e7.
21. Singhal, A.K., Cohen, B.I., Mosbach, E.H., Une, M., Stenger, R.J., McSherry, C.K., May-Donath, P., and Palaia, T. (1984). Prevention of cholesterol-induced gallstones by hyodeoxycholic acid in the prairie dog. J. Lipid Res. *25*, 539–549.
22. Shih, D.M., Shaposhnik, Z., Meng, Y., Rosales, M., Wang, X., Wu, J., Ratiner, B., Zadini, F., Zadini, G., and Lusis, A.J. (2013). Hyodeoxycholic acid improves HDL function and inhibits atherosclerotic lesion formation in LDLR-knockout mice. FASEB J. : official Publ. Fed. Am. Societies Exp. Biol. *27*, 3805–3817.
23. Sehayek, E., Ono, J.G., Duncan, E.M., Batta, A.K., Salen, G., Shefer, S., Neguyen, L.B., Yang, K., Lipkin, M., and Breslow, J.L. (2001). Hyodeoxycholic acid efficiently suppresses atherosclerosis formation and plasma cholesterol levels in mice. J. Lipid Res. *42*, 1250–1256.
24. Buras, J.A., Holzmann, B., and Sitkovsky, M. (2005). Animal models of sepsis: setting the stage. Nat. Rev. Drug Discov. *4*, 854–865.
25. Eyssen, H.J., De Pauw, G., and Van Eldere, J. (1999). Formation of hyodeoxycholic acid from muricholic acid and hyocholic acid by an unidentified gram-positive rod termed HDCA-1 isolated from rat intestinal microflora. Appl. Environ. Microbiol. *65*, 3158–3163.

26. Hur, H., and Rafii, F. (2000). Biotransformation of the isoflavonoids biochanin A, formononetin, and glycitein by Eubacterium limosum. FEMS Microbiol. Lett. *192*, 21–25.

27. Brown, R.L., Larkinson, M.L.Y., and Clarke, T.B. (2021). Immunological design of commensal communities to treat intestinal infection and inflammation. Plos Pathog. *17*, e1009191.

28. Costa, E.L.V., Schettino, I.A.L., and Schettino, G.P.P. (2006). The lung in sepsis: guilty or innocent? Endocr. Metab. Immune Disord. Drug Targets *6*, 213–216.

29. Kawai, T., and Akira, S. (2010). The role of pattern-recognition receptors in innate immunity: update on Toll-like receptors. Nat. Immunol. *11*, 373–384.

30. Hoshino, K., Takeuchi, O., Kawai, T., Sanjo, H., Ogawa, T., Takeda, Y., Takeda, K., and Akira, S. (1999). Cutting edge: toll-like receptor 4 (TLR4)-deficient mice are hyporesponsive to lipopolysaccharide: evidence for TLR4 as the Lps gene product. J. Immunol. *162*, 3749–3752.

31. Nagai, Y., Akashi, S., Nagafuku, M., Ogata, M., Iwakura, Y., Akira, S., Kitamura, T., Kosugi, A., Kimoto, M., and Miyake, K. (2002). Essential role of MD2 in LPS responsiveness and TLR4 distribution. Nat. Immunol. *3*, 667–672.

32. Ohto, U., Fukase, K., Miyake, K., and Shimizu, T. (2012). Structural basis of species-specific endotoxin sensing by innate immune receptor TLR4/MD2. Proc. Natl. Acad. Sci. USA *109*, 7421–7426.

33. Yang, T., Shu, T., Liu, G., Mei, H., Zhu, X., Huang, X., Zhang, L., and Jiang, Z. (2017). Quantitative profiling of 19 bile acids in rat plasma, liver, bile and different intestinal section contents to investigate bile acid homeostasis and the application of temporal variation of endogenous bile acids. J. Steroid Biochem. Mol. Biol. *172*, 69–78.

34. Petersen, A., Julienne, H., Hyötyläinen, T., Sen, P., Fan, Y., Pedersen, H.K., Jäntti, S., Hansen, T.H., Nielsen, T., Jørgensen, T., et al. (2021). Conjugated C-6 hydroxylated bile acids in serum relate to human metabolic health and gut Clostridia species. Sci. Rep. *11*, 13252.

35. Deo, A.K., and Bandiera, S.M. (2008). Biotransformation of lithocholic acid by rat hepatic microsomes: metabolite analysis by liquid chromatography/mass spectrometry. Drug Metab. Dispos. *36*, 442–451.

36. Einarsson, K. (1966). On the formation of hyodeoxycholic acid in the rat. Bile acids and steroids 154. J. Biol. Chem. *241*, 534–539.

37. Bodin, K., Lindbom, U., and Diczfalusy, U. (2005). Novel pathways of bile acid metabolism involving CYP3A4. Biochim. Biophys. Acta *1687*, 84–93.

38. Araya, Z., and Wikvall, K. (1999). 6alpha-hydroxylation of taurochenodeoxycholic acid and lithocholic acid by CYP3A4 in human liver microsomes. Biochim. Biophys. Acta *1438*, 47–54.

39. Wigner, P., Bijak, M., and Saluk-Bijak, J. (2022). Probiotics in the prevention of the calcium oxalate urolithiasis. Cells *11*.

40. Kuang, J., Zheng, X., Huang, F., Wang, S., Li, M., Zhao, M., Sang, C., Ge, K., Li, Y., Li, J., et al. (2020). Anti-adipogenic effect of theabrownin is mediated by bile acid alternative synthesis via gut microbiota remodeling. Metabolites *10*, 475.

41. Kosters, A., and Karpen, S.J. (2010). The role of inflammation in cholestasis: clinical and basic aspects. Semin. Liver Dis. *30*, 186–194.

42. Chen, T., Huang, W., Qian, J., Luo, W., Shan, P., Cai, Y., Lin, K., Wu, G., and Liang, G. (2020). Macrophage-derived myeloid differentiation protein 2 plays an essential role in ox-LDL-induced inflammation and atherosclerosis. EBioMedicine *53*, 102706.

43. Roger, T., Froidevaux, C., Le Roy, D., Reymond, M.K., Chanson, A.L., Mauri, D., Burns, K., Riederer, B.M., Akira, S., and Calandra, T. (2009). Protection from lethal gram-negative bacterial sepsis by targeting Toll-like receptor 4. Proc. Natl. Acad. Sci. USA *106*, 2348–2352.

44. Bruno, K., Woller, S.A., Miller, Y.I., Yaksh, T.L., Wallace, M., Beaton, G., and Chakravarthy, K. (2018). Targeting toll-like receptor-4 (TLR4)-an emerging therapeutic target for persistent pain states. Pain *159*, 1908–1915.

45. Zusso, M., Lunardi, V., Franceschini, D., Pagetta, A., Lo, R., Stifani, S., Frigo, A.C., Giusti, P., and Moro, S. (2019). Ciprofloxacin and levofloxacin attenuate microglia inflammatory response via TLR4/NF-kB pathway. J. Neuroinflammation *16*, 148.

46. Mian, M.F., Lauzon, N.M., Andrews, D.W., Lichty, B.D., and Ashkar, A.A. (2010). FimH can directly activate human and murine natural killer cells via TLR4. Mol. Ther. *18*, 1379–1388.

47. Mackenzie, P., Little, J.M., and Radominska-Pandya, A. (2003). Glucosidation of hyodeoxycholic acid by UDP-glucuronosyltransferase 2B7. Biochem. Pharmacol. *65*, 417–421.

48. Sabbatini, P., Filipponi, P., Sardella, R., Natalini, B., Nuti, R., Macchiarulo, A., Pellicciari, R., and Gioiello, A. (2013). Synthesis and quantitative structure-property relationships of side chain-modified hyodeoxycholic acid derivatives. Molecules (Basel, Switzerland) *18*, 10497–10513.

49. Singer, M., Deutschman, C.S., Seymour, C.W., Shankar-Hari, M., Annane, D., Bauer, M., Bellomo, R., Bernard, G.R., Chiche, J.D., Coopersmith, C.M., et al. (2016). The third international consensus definitions for sepsis and septic shock (Sepsis-3). Jama *315*, 801–810.

50. Fang, C., Zhong, H., Lin, Y., Chen, B., Han, M., Ren, H., Lu, H., Luber, J.M., Xia, M., Li, W., et al. (2018). Assessment of the cPAS-based BGISEQ-500 platform for metagenomic sequencing. GigaScience *7*, 1–8.

51. Chen, Y., Chen, Y., Shi, C., Huang, Z., Zhang, Y., Li, S., Li, Y., Ye, J., Yu, C., Li, Z., et al. (2018). SOAPnuke: a MapReduce acceleration-supported software for integrated quality control and preprocessing of high-throughput sequencing data. GigaScience *7*, 1–6.

52. Li, D., Liu, C.M., Luo, R., Sadakane, K., and Lam, T.W. (2015). MEGAHIT: an ultra-fast single-node solution for large and complex metagenomics assembly via succinct de Bruijn graph. Bioinformatics (Oxford, England) *31*, 1674–1676.

53. Wood, D.E., Lu, J., and Langmead, B. (2019). Improved metagenomic analysis with Kraken 2. Genome Biol. *20*, 257.

54. Wang, T., Zhang, X., Liu, Z., Yao, T., Zheng, D., Gan, J., Yu, S., Li, L., Chen, P., and Sun, J. (2021). Single-cell RNA sequencing reveals the sustained immune cell dysfunction in the pathogenesis of sepsis secondary to bacterial pneumonia. Genomics *113*, 1219–1233.

55. Zheng, G.X.Y., Terry, J.M., Belgrader, P., Ryvkin, P., Bent, Z.W., Wilson, R., Ziraldo, S.B., Wheeler, T.D., McDermott, G.P., Zhu, J., et al. (2017). Massively parallel digital transcriptional profiling of single cells. Nat. Commun. *8*, 14049.

56. Hao, Y., Hao, S., Andersen-Nissen, E., Mauck, W.M., 3rd, Zheng, S., Butler, A., Lee, M.J., Wilk, A.J., Darby, C., Zager, M., et al. (2021). Integrated analysis of multimodal single-cell data. Cell *184*, 3573–3587.e29.

57. Young, M.D., and Behjati, S. (2020). SoupX removes ambient RNA contamination from droplet-based single-cell RNA sequencing data. GigaScience *9*, giaa151.

58. McGinnis, C.S., Murrow, L.M., and Gartner, Z.J. (2019). DoubletFinder: doublet detection in single-cell RNA sequencing data using artificial nearest neighbors. Cell Syst. *8*, 329–337.e4.

59. Yu, G. (2018). Using meshes for MeSH term enrichment and semantic analyses. Bioinformatics (Oxford, England) *34*, 3766–3767.

60. Hänzelmann, S., Castelo, R., and Guinney, J. (2013). GSVA: gene set variation analysis for microarray and RNA-seq data. BMC bioinformatics *14*, 7.

61. Sun, S., He, M., Wang, Y., Yang, H., and Al-Abed, Y. (2018). Folic acid derived-P5779 mimetics regulate DAMP-mediated inflammation through disruption of HMGB1:TLR4:MD2 axes. PLoS one *13*, e0193028.

62. Xing, J., Li, R., Li, N., Zhang, J., Li, Y., Gong, P., Gao, D., Liu, H., and Zhang, Y. (2015). Anti-inflammatory effect of procyanidin B1 on LPS-treated THP1 cells via interaction with the TLR4-MD2 heterodimer and p38 MAPK and NF-κB signaling. Mol. Cell. Biochem. *407*, 89–95.